

## THE LUMINOSITY FUNCTION OF *IRAS* PSCZ GALAXIES

TSUTOMU T. TAKEUCHI<sup>1,2</sup>, KOHJI YOSHIKAWA<sup>3</sup>, AND TAKAKO T. ISHII<sup>4</sup>

*Draft version November 3, 2018*

### ABSTRACT

We estimated the luminosity function (LF) of *IRAS* galaxies in the PSCz catalogue. The faint end of the PSCz LF is slightly steeper than that of the LF derived by Saunders et al. (1990; S90). Using an analytical form for the LF used by S90, we obtain the following parameters:  $\alpha = 1.23 \pm 0.04$ ,  $L_* = (8.85 \pm 1.75) \times 10^8 h^{-2} L_\odot$ ,  $\sigma = 0.724 \pm 0.010$ , and  $\phi_* = (2.34 \pm 0.30) \times 10^{-2} h^3 \text{Mpc}^{-3}$ . We also examined the evolution in the sample by a simple assumption  $\phi_*(z) \propto (1+z)^P$ , and found  $P = 3.40 \pm 0.70$ . It does not affect the three parameters,  $\alpha$ ,  $L_*$ , and  $\sigma$ , but  $\phi_*(z=0)$  is overestimated up to  $\sim 15\%$  if we ignore evolution. We estimated the temperature dependence of the LF. The LFs of warm and cool galaxies are quite different: the LF of warm galaxies has a very steep faint end with  $\alpha = 1.37$ . We also discuss a lump found at the brightest end of the LF.

*Subject headings:* galaxies: luminosity function, mass function — galaxies: statistics — infrared: galaxies — methods: statistical

### 1. INTRODUCTION

Galaxy luminosity function (LF) is an important tool to characterize the statistical properties of galaxies. The far-infrared (FIR) LF enables us to evaluate the properties of interstellar dust and its heating sources in various galaxy populations. The Infrared Astronomical Satellite (*IRAS*) has provided us a uniform FIR all-sky survey of local galaxies. In addition to its own importance, the FIR LF has also come to the limelight in conjunction with the evolution of FIR galaxies. Evaluation of their evolution plays a crucial role in understanding the cosmic star formation history hidden by dust (e.g., Franceschini et al. 2001; Takeuchi et al. 2001a,b; Rowan-Robinson 2001; Granato et al. 2000; Totani & Takeuchi 2002; Takeuchi, Shibai, & Ishii 2002).

In spite of many attempts to estimate the LF of *IRAS* galaxies (e.g., Lawrence et al. 1986; Soifer et al. 1987; Saunders et al. 1990 (S90); Isobe & Feigelson 1992), there is yet room for improvement in its exact shape, especially at the faint end. The best way to overcome this difficulty is, of course, a statistical analysis of a huge homogeneous dataset.

The PSCz catalogue (Saunders et al. 2000) (S00) is the largest well controlled redshift sample of *IRAS* galaxies to date. The catalogue is complete to 0.6 Jy at 60  $\mu\text{m}$  and contains 15411 *IRAS* galaxies covering 84 % of the sky. This is an ideal dataset to estimate the exact shape of the LF of *IRAS* galaxies.

In this *Letter*, we estimate the LF from the PSCz catalogue using the statistical package for LF estimation developed by us (Takeuchi, Yoshikawa, & Ishii 2000; hereafter T00) and examine the exact shape of the FIR LF. We use the cosmological parameter set  $(h, \Omega_0, \lambda_0) = (0.7, 0.3, 0.7)$  except otherwise stated.

### 2. ANALYSIS

#### 2.1. Data Description

##### 2.1.1. Flux density

The data provided by S00 include (1) PSC flux, (2) point-source-filtered ADDSCAN flux, and (3) extended (coadded or extended ADDSCAN) flux for all the sources. First we should

note that the flux densities of nearby extended sources can be seriously underestimated because of the fixed aperture of *IRAS*. Indeed, Figure 2 of S00 shows a clear trend of underestimation in PSC flux or point-source-filtered flux. We used (3), coadded or extended ADDSCAN flux, that has been carefully measured and homogenized by S00.

##### 2.1.2. Local Group galaxies

The main catalog of S00 explicitly excludes the Local Group (LG) galaxies, and they are separately compiled in another catalog ‘*ilg.dat*’. There is a possibility that the exclusion of these galaxies slightly affects the faintest-end slope estimate of the LF, because they generally have low luminosities. In order to include the LG galaxies we adopted the distances presented by van den Bergh (2000), adjusted for the cosmological parameters used. We compared the LFs estimated from the datasets with and without LG galaxies, and obtained completely the same results: their inclusion caused no difference at all. For Virgo infall correction, we adopted a flow model very similar to model V3 of S90.

### 2.2. *K*-correction

To make *K*-correction, we used extended fluxes of  $S_{25}$ ,  $S_{60}$ , and  $S_{100}$  tabulated in the PSCz catalogue and fitted a 2nd-order polynomial to the flux densities for each galaxy:

$$\log \tilde{S}_\lambda(\log \lambda) = \sum_{i=0}^2 a_i (\log \lambda)^i, \quad (1)$$

$$\log S_{60}^{\text{em}} = \log \tilde{S}_{[60(1+z)]} \quad (2)$$

where  $\tilde{S}_\lambda$  is the interpolated flux density at wavelength  $\lambda \mu\text{m}$ , superscript ‘em’ means that the flux is measured at the emitted wavelength, and coefficients  $a_i$  are estimated from the observed fluxes  $S_{25}$ ,  $S_{60}$ , and  $S_{100}$ .

<sup>1</sup>National Astronomical Observatory of Japan, Mitaka, Tokyo 181–8588, JAPAN; takeuchi@optik.mtk.nao.ac.jp.

<sup>2</sup>Research Fellow of the Japan Society for the Promotion of Science

<sup>3</sup>Research Center for the Early Universe (RESCEU), The University of Tokyo, Bunkyo-ku, Tokyo 113–0033, JAPAN; kohji@utap.phys.s.u-tokyo.ac.jp.

<sup>4</sup>Kwasan and Hida Observatories, Kyoto University, Yamashina-ku, Kyoto 607–8471, JAPAN; ishii@kwasan.kyoto-u.ac.jp.

### 2.3. Statistical Methods

T00 extensively discussed four nonparametric statistical methods for estimating galaxy LF. The methods are 1)  $1/V_{\max}$  method (Schmidt 1968; Eales 1993), 2) Efstathiou, Ellis, & Peterson (1988) (EEP) method, 3) Chołoniewski (1986) method, and 4) improved  $C^-$  method (Lynden-Bell 1971; Chołoniewski 1987). The associated error is estimated by a bootstrap resampling (see T00). Equation (3) has been verified to be appropriate for a FIR LF (see Appendix D of S90). Hence, in Section 3 we also show the parametric fit for the LF by the parameter estimation advocated by Sandage, Tammann, & Yahil (1979), using

$$\phi(L) = \phi_* \left( \frac{L}{L_*} \right)^{1-\alpha} \exp \left[ -\frac{1}{2\sigma^2} \left\{ \log \left( 1 + \frac{L}{L_*} \right) \right\}^2 \right]. \quad (3)$$

We note that, while the  $C^-$ , EEP, and the Chołoniewski methods are robust against density fluctuation, the  $1/V_{\max}$  method is not accurate if a density inhomogeneity exists in the sample, as pointed out by previous studies.

### 3. THE PSCZ LUMINOSITY FUNCTION

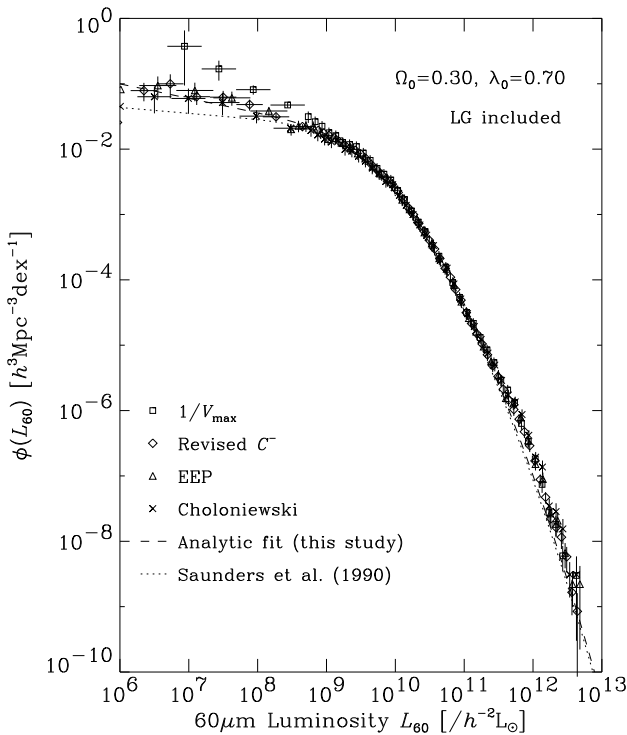


FIG. 1.— The luminosity function (LF) of *IRAS* PSCz galaxies. The squares, diamonds, triangles, and crosses represent the results obtained with  $1/V_{\max}$ , improved  $C^-$ , EEP, and Chołoniewski methods, respectively. The faint-end estimates ( $10^6$ – $10^9 L_{\odot}$ ) are rebinned to reduce statistical fluctuation. The dashed line describes the analytic LF derived in this work. The parametric result of Saunders et al. (1990) is also shown by the dotted line.

Figure 1 is the FIR LF of the PSCz catalogue. Different symbols represent the results obtained by different estimators. The dashed line describes the analytic LF derived in this work. The parametric solution of S90 is also shown in Figure 1 by the dotted line. We see that the estimates by the three inhomogeneity-insensitive methods show excellent agreement with one another, and at a faint regime  $L_{60} \lesssim 10^9 L_{\odot}$ ,  $1/V_{\max}$  estimate

significantly deviates upward because of the local density enhancement. We note that LG galaxies are included in the sample to produce Figure 1.

S90 proposed the following values for Equation (3):  $\alpha = 1.09 \pm 0.120$ ,  $L_* = (2.95^{+2.06}_{-1.21}) \times 10^8 h^{-2} L_{\odot}$ ,  $\sigma = 0.724 \pm 0.031$ , and  $\phi_* = (2.6 \pm 0.8) \times 10^{-2} h^3 \text{ Mpc}^{-3}$ . These values were obtained from the compiled redshifts of 2818 *IRAS* galaxies. We find that the bright end of the PSCz LF is remarkably well described by the analytic form estimated by S90. The normalization also nicely agrees with that of S90. At this stage we ignore the possible effect of galaxy evolution, which we will discuss in Section 5.1.2.

However, the faint end deviates from the result of S90. The three inhomogeneity-insensitive estimates show consistently the same trend. Hence the steep faint end of the PSCz LF is not caused by density enhancement, and we conclude that it is an intrinsic statistical property of the local *IRAS* galaxies.

We also estimated parameters for the analytic fit expressed by Equation (3) as follows:

$$\begin{aligned} \alpha &= 1.23 \pm 0.04, \\ L_* &= (8.85 \pm 1.75) \times 10^8 h^{-2} [L_{\odot}], \\ \sigma &= 0.724 \pm 0.01, \\ \phi_* &= (2.60 \pm 0.30) \times 10^{-2} h^3 [\text{Mpc}^{-3}]. \end{aligned} \quad (4)$$

The uncertainty for each parameter is estimated from the relative marginalized logarithmic likelihood. The log-likelihood around the maximum likelihood solution asymptotically behaves like a Gaussian, hence we can estimate  $1\text{-}\sigma$  error from  $\Delta \ln \mathcal{L} \equiv \ln \mathcal{L} - \ln \mathcal{L}_{\max} = -0.5$ . We note that  $\alpha$  is larger than that of S90 (3-sigma significant), though within their quoted error, it is consistent with the estimate of S90. The large  $\alpha$  quantitatively describes the above-mentioned steep faint end. On the other hand, we obtain almost the same value for  $\sigma$ , which characterizes the bright-end shape, and  $\phi$ , which determines the density normalization.

### 4. THE LUMINOSITY FUNCTION OF WARM AND COOL *IRAS* GALAXIES

In this section we derive the LFs of relatively warm and cool galaxies in the PSCz sample of galaxies. We chose the boundary of these classes to be  $\beta = S_{100}/S_{60} = 2.1$ , which is almost the median value for the sample. Helou (1986) has discussed the color–color diagram of normal *IRAS* galaxies. From his Figure 1, we find that  $\beta = 2.1$  is also equal to the median of his sample. If we use a modified blackbody with emissivity index 1.5,  $\beta = 2.1$  corresponds to the dust temperature  $\sim 25$  K. We refer to the galaxies with  $\beta \leq 2.1$  as ‘warm galaxies’, and those with  $\beta > 2.1$  as ‘cool galaxies’ in this study.

S00 have assigned extended ADDSCAN fluxes to all galaxies, we simply used these values to estimate  $\beta$ . However, warmer galaxies tend to have larger luminosities (e.g., Takeuchi et al. 2001a), this procedure might introduce a complex selection bias. We reconstruct the complete subsample of each category by adopting a shallower flux limit of  $S_{60} \geq 0.912$  Jy. The final sizes of the two samples are 5554 (warm) and 3421 (cool).

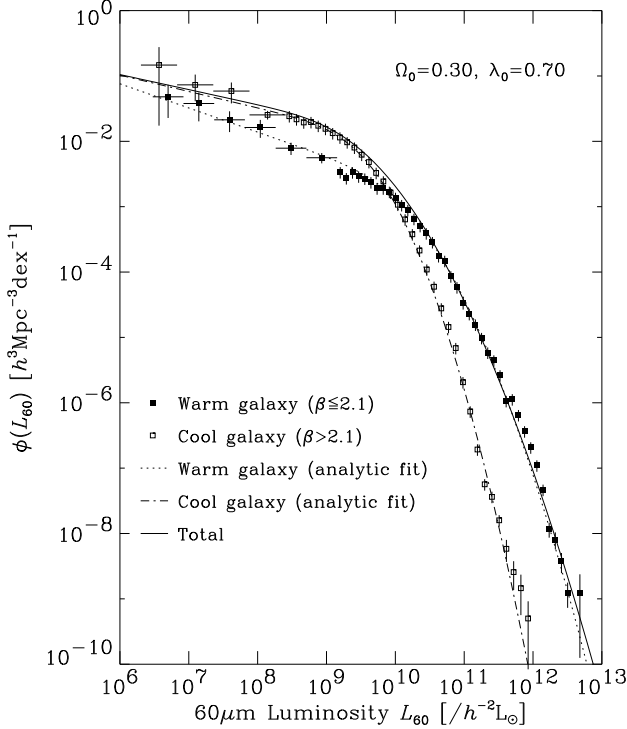


FIG. 2.— The luminosity function (LF) of warm ( $\beta \leq 2.1$ ) and cool ( $\beta > 2.1$ ) galaxies. The solid curve describes the analytic expression of the LF of the whole PSCz galaxies. Filled and open squares represent the LFs of warm and cool galaxies, respectively. Dotted and dot-dashed lines depict the analytic fits of the warm and cool galaxies.

The LFs of the warm and cool PSCz galaxies are shown in Figure 2. In Figure 2, we show only the estimates by EEP method for clarity; but the other estimates show a good agreement with one another. The parameters of the analytic fit for warm galaxies are

$$\begin{aligned} \alpha &= 1.37 \pm 0.05, \\ L_* &= (5.10 \pm 0.90) \times 10^9 h^{-2} [L_\odot], \\ \sigma &= 0.625 \pm 0.015, \\ \phi_* &= (4.20 \pm 0.85) \times 10^{-3} h^3 [\text{Mpc}^{-3}], \end{aligned} \quad (5)$$

and those for cool galaxies are

$$\begin{aligned} \alpha &= 1.25 \pm 0.06, \\ L_* &= (1.95 \pm 0.40) \times 10^8 h^{-2} [L_\odot], \\ \sigma &= 0.500 \pm 0.020, \\ \phi_* &= (1.85 \pm 0.37) \times 10^{-2} h^3 [\text{Mpc}^{-3}]. \end{aligned} \quad (6)$$

We also show the analytic fits for these two groups in Figure 2. S90 performed a similar analysis of warm and cool galaxies. They first fit modified blackbody spectra to *IRAS* flux data and defined dust temperature, and then divide the sample into galaxies with  $T \geq 36$  K and  $T < 36$  K. Though they give systematically higher temperature than ours, their LF of each class is quite similar to ours; therefore, S90 and we probably treat nearly the same populations.

It is interesting to note that the faintest end of the warm galaxies increases steeply. This means that a significant fraction of galaxies at luminosities  $L_{60} \lesssim 10^7 L_\odot$  can be low-luminosity but hot galaxies. Because of their low luminosity, detailed case studies of their spectral energy distributions and next generation large FIR surveys (e.g., *ASTRO-F*, *SIRTF*, and *Herschel*) are important to reveal their physical properties.

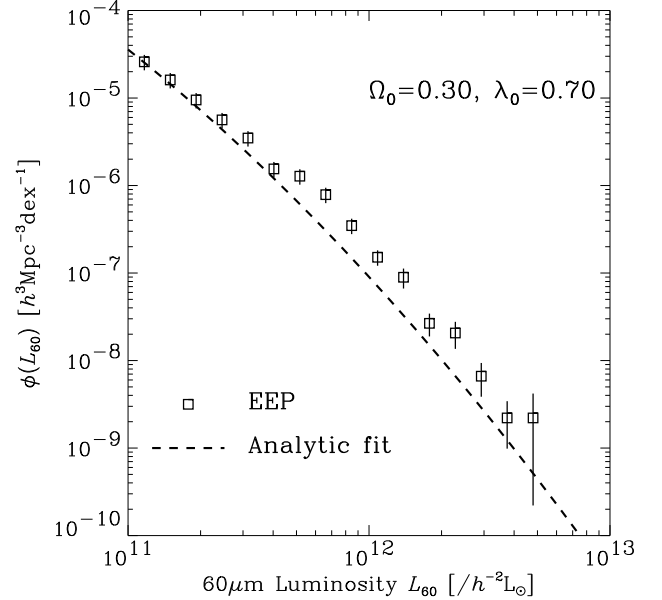


FIG. 3.— The zoom-up of the bright-end of the luminosity function. We only plot EEP estimates for clarity. A significant lump is found at luminosity  $L_{60} \gtrsim 10^{11.5} L_\odot$ .

## 5. DISCUSSION

### 5.1. Possible Systematic Uncertainties in LF Parameters

#### 5.1.1. Hubble constant

We further consider some subtle effects on the parameter estimation. The effect of the choice of cosmological parameters is examined in S90. Their Figure 5 illustrates the dependence of the estimated LF. We should be cautious that the faint end slope is slightly affected by the choice of the Hubble constant,  $h$ . But according to their Figure 5, if we use larger  $h$ , the estimated  $\alpha$  will be smaller. Hence, our steep faint-end slope is not due to this effect.

#### 5.1.2. Evolution

Rowan-Robinson (2001) mentions the possibility that the parameters are affected by galaxy evolution of the sample. Hence we examined this issue by dividing the whole sample into  $z < 0.02$  and  $z > 0.02$  groups. We derived the LF of each group and found that the faint end of the LF of the total PSCz sample is dominated by galaxies at  $z < 0.02$ . The flux density limit of 0.6 Jy corresponds to  $L_{60} \sim 10^{9.6} L_\odot$  at  $z = 0.02$  ( $h = 0.7$ ), therefore the evolution toward higher redshift can hardly affect the estimation of  $\alpha$ .

On the other hand, evolution may affect the estimation of the normalization of the LF. We estimated the evolution strength under the assumption  $n(z) \propto n_0(1+z)^P$ , where  $n_0$  and  $n(z)$  is the comoving number density of galaxies at redshift 0 and  $z$ , respectively (S90). If we assume that the LF is separable for  $L$  and  $z$  as  $\phi(L, z) = n(z)p(L)$ , then the likelihood is expressed as

$$\begin{aligned} \mathcal{L}(P|\{(L_i, z_i)\}_{i=1, \dots, N}) &= \prod_{i=1}^N \frac{n(z_i)p(L_i)}{\int n(z)p(L_i)(dV/dz)dz} \\ &= \prod_{i=1}^N \frac{(1+z_i)^P}{\int_0^{z_{\max, i}} (1+z)^P (dV/dz)dz}, \quad (7) \end{aligned}$$

where  $p(L)$  denotes the probability density for a galaxy having a luminosity  $L$ , and  $z_{\max,i}$  represents the maximum redshift to which a galaxy  $i$  can be detected within the flux limit  $S_{\text{lim}}$ . We can estimate the strength of density evolution,  $P$ , by maximizing the above likelihood equation [Equation (7)].

We obtained  $P = 3.40 \pm 0.70$ . This value is much smaller than that estimated by S90, but consistent with the estimate of Springel & White (1998). By using this value, we found that the density normalization  $\phi_*(z=0)$  is overestimated up to  $\sim 10\text{--}15\%$  if evolution is ignored. This systematic error is comparable to the statistical uncertainty of  $\sim 12\%$ . Thus, the density normalization parameter is  $\phi_* = 2.34$  if we properly take into account the evolution.

### 5.2. Bright End Population

It is worthwhile to note the lump found in the bright end of the LF in Figure 1 at  $L_{60} \gtrsim 10^{11.5} L_{\odot}$ . The zoom-up of the bright-end is shown in Figure 3. We only plot EEP estimates for clarity. We consider which population of galaxies dominates

the high-luminosity lump. Machalski & Godlowski (2000) presented the radio (1.4 GHz) LF from UGC (Nilson 1973) and LCRS (Shectman et al. 1996) galaxy samples. Their radio LF clearly shows that it consists of two distinct populations: star-forming galaxies and AGNs. At  $L_{1.4\text{GHz}} > 10^{23.4} [\text{WHz}^{-1}]$  AGN contribution dominates the LF. We can convert the radio luminosity to FIR one by the well-known radio-FIR correlation (Condon 1992) and obtain the corresponding  $L_{\text{FIR}} \simeq 5.0 \times 10^{11} L_{\odot}$ . It agrees with the  $60\text{-}\mu\text{m}$  luminosity at which the lump begins to appear. So we suggest that the AGN contribution is attributed to the lump of the LF at  $L_{60} \gtrsim 10^{11.5} L_{\odot}$ . Different energetics may be the cause of discontinuity in the LF shape. It is interesting that both warm and cool galaxies show departure from the analytic fit at the same  $L_{60}$  (see Figure 2).

We thank two referees for thoughtful comments and scrutiny that have improved the quality of this paper very much. We also thank H. Hirashita, T. N. Rengarajan, and M. Imanishi who gave us useful suggestions. TTT has been supported by JSPS.

### REFERENCES

- Choloniewski, J. 1986, MNRAS, 223, 1  
 Choloniewski, J. 1987, MNRAS, 226, 273  
 Condon, J. J. 1992, ARA&A, 30, 575  
 Eales, S. 1993, ApJ, 404, 51  
 Efstathiou, G., Ellis, R. S., & Peterson, B. A. 1988, MNRAS, 232, 431 (EEP)  
 Granato, G. L., Lacey, C. G., Silva, L., Bressan, A., Baugh, C. M., Cole, S., & Frenk, C. S. 2000, ApJ, 542, 710  
 Franceschini, A., Aussel, H., Cesarsky, C. J., Elbaz, D., & Fadda, D. 2001, A&A, 378, 1  
 Helou, G. 1986, ApJ, 311, L33  
 Isobe, T., & Feigelson, E. 1992, ApJS, 79, 197  
 Lawrence, A., Walker, D., Rowan-Robinson, M., Leech, K. J., & Penston, M. V. 1986, MNRAS, 219, 687  
 Lynden-Bell, D. 1971, MNRAS, 155, 95  
 Machalski, J., & Godlowski, W. 2000, A&A, 360, 463  
 Nilson, P. 1973, Uppsala General Catalogues of Galaxies, Uppsala Astronomical Observatory (UGC)  
 Rowan-Robinson, M. 2001, ApJ, 549, 745  
 Sandage, A., Tammann, G. A., & Yahil, A. 1979, ApJ, 232, 352  
 Saunders, W., Rowan-Robinson, M., Lawrence, A., Efstathiou, G., Kaiser, N., Ellis, R. S., & Frenk, C. S. 1990, MNRAS, 242, 318 (S90)  
 Saunders, W., et al. 2000, MNRAS, 317, 55 (S00)  
 Schmidt, M. 1968, ApJ, 151, 393  
 Shectman, S. A., Landy, S. D., Oemler, A., Jr., Tucker, D. L., Lin, H., Kirshner, R. P., & Schechter, P. L. 1996, ApJ, 470, 172  
 Soifer B. T., Sanders, D. B., Madore, B. F., Neugebauer, G., Danielson, G. E., Elias, J. H., Lonsdale, C. J., & Rice, W. L. 1987, ApJ, 320, 238  
 Springel, V., & White, S. D. M. 1998, MNRAS, 298, 143  
 Takeuchi, T. T., Yoshikawa, K., & Ishii, T. T. 2000, ApJS, 129, 1 (T00)  
 Takeuchi, T. T., Ishii, T. T., Hirashita, H., Yoshikawa, K., Matsuhara, H., Kawara, K., & Okuda, H. PASJ, 2001a, 53, 37  
 Takeuchi, T. T., Kawabe, R., Kohno, K., Nakanishi, K., Ishii, T. T., Hirashita, H., & Yoshikawa, K. 2001b, PASP, 113, 586  
 Takeuchi, T. T., Shibai, H., & Ishii, T. T. 2002, Adv. Space Res., 30, 2021  
 Totani, T., & Takeuchi, T. T. 2002, ApJ, 570, 470  
 van den Bergh, S. 2000, The Galaxies of the Local Group, Cambridge University Press, Cambridge